Talanta 126 (2014) 82–90

Contents lists available at ScienceDirect

Talanta

journal homepage: www.elsevier.com/locate/talanta

A thermostated electrochemical flow cell with a coupled bismuth film electrode for square-wave anodic stripping voltammetric determination of cadmium(II) and lead(II) in natural, wastewater and tap water samples

Vagner B. dos Santos [a], Elson L. Fava [a], Newton S. de Miranda Curi [b], Ronaldo C. Faria [a], Orlando Fatibello-Filho [a,*]

[a] Departamento de Química, Centro de Ciências Exatas e de Tecnologia, Universidade Federal de São Carlos, Caixa Postal 676, CEP 13560-970 São Carlos, SP, Brazil
[b] FAC, Cândido de Arruda Botelho, São Carlos, SP, Brazil

ARTICLE INFO

Article history:
Received 30 January 2014
Received in revised form
4 March 2014
Accepted 11 March 2014
Available online 19 March 2014

Keywords:
Bismuth film electrode
Screen-printed electrode
Flow-batch analysis
Thermostated control
Electrochemical flow cell

ABSTRACT

In order to reduce the sample consumption and waste generation for electrochemical purposes, a screen-printed electrode (SPE) used for electrodeposition of bismuth film (SPE-BiFE) and a thermostated electrochemical flow cell (EFC) were developed. The SPE-BiFE with the EFC was employed to determine Cd^{2+} and Pb^{2+} ions in natural, wastewater and tap water samples by square-wave anodic stripping voltammetry (SWASV). For this, the flow-batch analysis (FBA) approach based on solenoid micro-pumps and three-way valves was developed to carry out a fully automated procedure with temperature control. Furthermore, the FBA and the SWASV parameters were optimized, on line simultaneous determination of Cd^{2+} and Pb^{2+} ions was performed and two analytical curves were linearly acquired in the concentration ranges from 6.30 to 75.6 $\mu g\,L^{-1}$ and from 3.20 to 38.4 $\mu g\,L^{-1}$, respectively. Moreover, limits of detection of 0.60 $\mu g\,L^{-1}$ and 0.10 $\mu g\,L^{-1}$ for Cd^{2+} and Pb^{2+}, respectively, were obtained. Studies of precision for the same SPE-BiFE and repeatability for five built SPE-BiFE were carried out for Cd^{2+} and Pb^{2+} ion measurements and RSD of 4.1% and 2.9% ($n=3$) with repeatabilities ($n=5$) of 6.5% and 8.0% were respectively obtained for both analytes. Besides, a low consumption of 700 μL of reagents and a sampling frequency of 13 h^{-1} were acquired. Simplicity, fast response, accuracy, high portability, robustness and suitability for *in loco* analyses are the main features of the proposed electroanalytical method.

1. Introduction

According to green chemistry and environmentally-friendly research, electrochemical and electroanalytical experiments have to advance in order to reduce the generation of waste and chemical consumption [1]. To reach this goal, a miniaturization of the apparatus and/or devices seems to be moving forwards. In this context, different models of electrochemical cells and electrodes have been widely developed and described in the literature [2]. For this purpose, the use of miniaturized electrodes such as screen-printed electrodes (SPE) or microelectrodes is desired. In fact, these kinds of electrodes are simple, practical, efficient and low-cost when compared to the conventional electrodes that are currently on the market [3].

SPEs are interesting because of their cost-effectiveness, since they can be manufactured on a large scale whilst minimizing production costs and they can also be properly disposed of. There are many types sold commercially: carbon graphite electrodes, bismuth film electrodes (BiFE), carbon nanotubes, and carbon nanotubes modified with enzymes (biosensors) [4]. Among these electrodes, BiFE has also been used and provides good repeatability, low residual current and high hydrogen overpotential [5]. Moreover, BiFE has the ability to form alloys at room temperature with some metal cations such as Cd^{2+}, Co^{2+}, Ni^{2+}, Sn^{2+}, Ga^{2+}, Tl^{+}, Zn^{2+} and Pb^{2+}, allowing its determination in low concentrations, especially when anodic stripping voltammetry (ASV) has been applied [5–9]. In addition, its low toxicity and low sensitivity to dissolved oxygen in samples are very important for *in loco* determinations [10].

The main advantage of using these electrodes is the possibility of the miniaturization of the electrochemical cell [11], because the

* Corresponding author. Tel.: +55 16 33518098; fax: +55 16 33518350.
E-mail address: bello@ufscar.br (O. Fatibello-Filho).

http://dx.doi.org/10.1016/j.talanta.2014.03.015
0039-9140/

size of these cells is a few milliliters or microliters, making them very attractive from economic and, in particular, environmental points of view. In this context, Noyhouzer and Mandler [2], Economou and Voulgaropoulos [8], Chuanuwatanakul et al. [12], Henriquez et al. [13] and Ninwong et al. [14] demonstrated the use of SPE with EFC and flow analysis techniques, especially flow injection analysis (FIA) and sequential injection analysis (SIA) with ASV as the detection technique. In general, these procedures presented a sampling rate from 10 to 20 samples per hour, low waste generation from 800 to 1200 μL and low limits of detection in the range from 0.1 to 10 μg L^{-1} when applying anodic stripping voltammetry (ASV) for the determination of Pb^{2+} and Cd^{2+}. Among these methods, several advantages were obtained such as the minimal handling of solutions, good accuracy, and lower consumption of reagents. Consequently, these approaches reduce the cost per analysis compared to non-automated analyses [15,16].

A multicommutation in flow analysis (MCFA) proposed by Reis et al. [17] is another flow approach which is widely applied in automated analytical methods. In MCFA, the multicommutation can be performed by controlling the switch on the three-way solenoid valves (SV) while a propulsion unit (*i.e.* peristaltic pump) is switched on. Another alternative is based on controlling the solenoid micropumps (μP) as the propulsion device. By using the μP, the solutions are selected and inserted into the carrier solution (supporting electrolyte) of the flow system by controlling the pulsation frequency. Moreover, in MCFA, distinct apparatus can be inserted along the flow path, such as a mixture chamber. This kind of chamber characterizes a flow method named flow-batch analyses (FBA), which was developed by Honorato et al. [18]. By using this apparatus, constructions of analytical curves, standard addition methods, dilutions, and recovery studies can be easily performed with better homogenization, mainly due to the use of the mixture chamber.

In the literature, the *in loco* determination, especially in environmental experiments, is encouraged. This kind of analysis is important; however, there are few researches performing procedures in the field, due to difficult environmental conditions, especially temperature variations during the analyses [19]. The temperature variation during experiments *in loco* can lead to very unsatisfactory results [20]. In electrochemical and/or electroanalytical experiments, temperature variations can affect the enzyme activity in biosensors [21], repeatability in the production of thin films, variations in diffusion coefficients and/or the mobility of the species and/or analytes in solution [22,23]. Furthermore, the generation of a temperature gradient between the electrode surface and the bulk of the solution can significantly affect the mass transport, acting strongly on the diffusion of analytes [24].

To overcome this drawback, a thermostated EFC was developed to control the temperature of samples during the ASV determinations. For this, an FBA system based on solenoid μPs was constructed for the on line and *ex situ* electrochemical deposition of bismuth film and posteriorly to determine Pb^{2+} and Cd^{2+} in natural, wastewater and tap water samples by SWASV, employing the screen-printed electrode based on bismuth which was developed for this purpose.

2. Experimental

2.1. Chemicals and samples acquisition

The buffer solutions acetic acid/acetate (0.2 mol L^{-1} pH 4.0 and pH 4.5), phosphate (0.2 mol L^{-1} pH 4.0 and pH 4.5) and Britton–Robinson (BR) (0.4 mol L^{-1}, pH 2.0, 4.0 and 6.0) were prepared and used in the supporting electrolyte studies. Solutions of 0.02 mol L^{-1} $Bi(NO_3)_3 \cdot 5H_2O$ in 0.15 mol L^{-1} sodium citrate and 1.5 mol L^{-1} HCl were used for the electrochemical deposition of bismuth film [25]. Solutions of certified metal ions were from the NIST (National Institute of Standards and Technology) (USA), and 1000 mg L^{-1} of Pb^{2+} and Cd^{2+} dissolved in 0.1 mol L^{-1} HNO_3 were purchased from Merck® (Germany). Appropriate dilutions of these standard solutions were prepared using acetic acid/acetate (0.2 mol L^{-1} pH 4.0 and pH 4.5) buffer solutions. A certified river water (1643e Trace Elements in Water, NIST) contain 6.58 ± 0.073 μg L^{-1} Cd^{2+} and 19.63 ± 0.21 μg L^{-1} Pb^{2+} ions was used for accuracy tests. Deionized water (resistivity > 1.8 MΩ cm) obtained from a Milli-Q system (Millipore®, USA) was used. Furthermore, all reagents used were of analytical grade purchased from Acros® (USA), Sigma® (USA) and Merck® (Germany).

The water samples were collected from the Monjolinho Lake in São Carlos (Brazil) at three distinct points. Some samples were directly collected from the tap through the water distribution system in São Carlos (Brazil), Lisbon (Portugal) and Alicante (Spain). Other samples were obtained from the pretreatment from the water substations (SANEPAR, Brazil), from wastewater from the petrochemical industry (Petrobras®, Brazil), and from the Fatima source in Alicante (Spain).

The samples were previously collected in decontaminated flasks cleaned with a solution of 15% (v/v) HNO_3, packed in Styrofoam and maintained between −5 and 5 °C. Then, all samples were filtered through 0.45 μm filter paper (Whatman®, USA) using a vacuum pump.

2.2. Instruments and apparatus

The electroanalytical data were obtained using a portable potentiostat/galvanostat (Uniscan®, England) managed by UiEChen® software. Six solenoid micropumps (μP), model 120SP1220 (Coleparmer®, USA), with a pumping capacity of 20 μL per pulse and three-way SV (Neptune Research®, USA), model 161TO31, were used. For the activation of μPs and SV, an actuator board was designed to provide 12 VDC (direct current). This circuit was driven by a USB interface model 6008 from National Instruments (NI®, USA) in which it was coupled to a notebook (Semp Toshiba®, Japan) model IS 1414 and controlled by software developed in Labview® Professional 2011 (NI®, USA). The polytetrafluoroethylene (PTFE) flow transmission lines with 0.8 mm i.d. and the two-way connectors of Teflon® were used. A thermoelectric cell (Danvic®, Brazil), model HTC-40-03-15.4, a 12 V rechargeable battery with 7000 mA h^{-1} (Unipower®, Brazil), a microcontroller PIC 18F4550 model (Microchip®, USA), and an LM35 temperature sensor (Texas Instruments®, USA) were used [21]. A heat press, model PTM 30 (Brazil) was used for the production of the screen-printed electrodes. The counter electrode (CE) and the pseudo-reference (pseudo-RE) were fabricated using conductive graphite ink and conductive silver epoxy resin (Electron Microscopy Sciences®, USA), respectively. The other parts of the SPE were fabricated using copper from printed circuit boards (PCB).

2.3. SPE used for electrodeposition of bismuth film

The screen-printed technology was employed in fabrication the electrodes [26], where some units were produced in the same lot. The procedure was illustrated in scheme presented in Fig. 1.

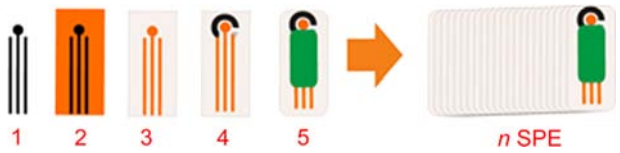

Fig. 1. Sequence used to prepare the SPEs.

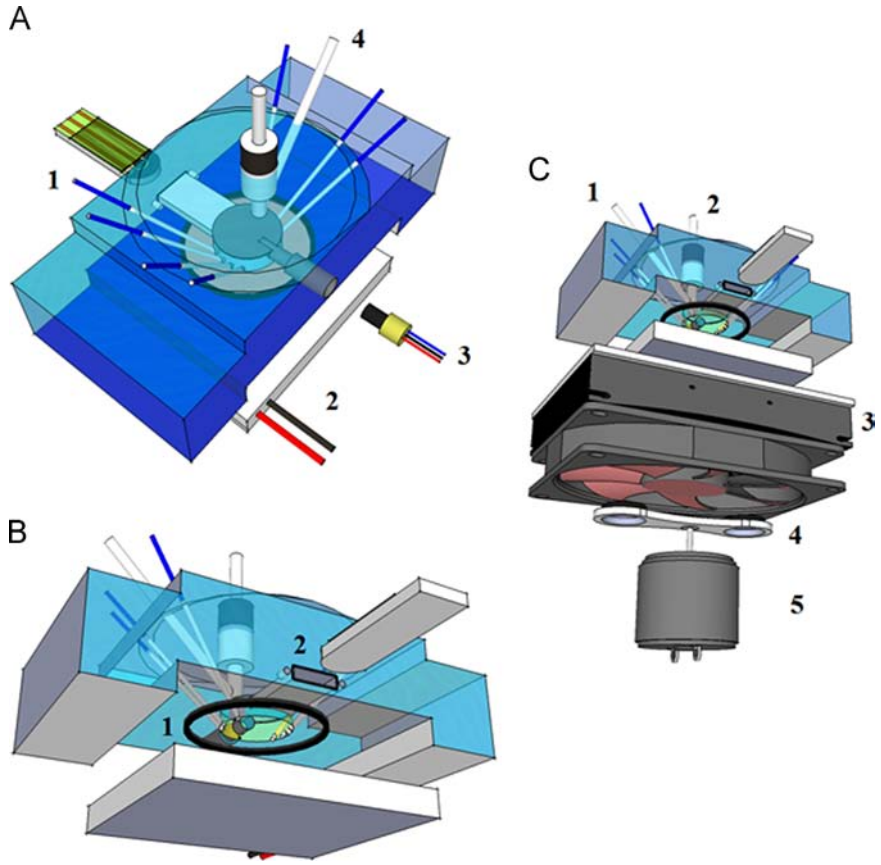

Fig. 2. Thermostated EFC design. PTFE tube with 0.8 mm i.d. coupled to the EFC used for inlet flow (1), TEC-Peltier (2), temperature sensor (3) and the blank Tygon® tube or an external CE with 3.0 mm i.d. used as the outlet flow (4) (A). Inside view from the bottom up of the EFC with details of the O-rings used to seal the base of the EFC (1) and the SPE (2) (B). Tygon® tube or an external CE (1), an external RE (Ag/AgCl (3.0 mol L^{-1} KCl)) (2), a TEC-Peltier with a heat dissipation system composed of an aluminum block and a fan (3), a pair of magnets (4) coupled to a motor axis (5) for mechanical agitation (C).

The design was developed in Coreldraw X3® (step 1) and printed on transfer paper with a toner from a laser printer (HP Laser Jet P2035n) and moved to a PCB by heating at 200 °C for 4 min (step 2). Then, the copper layer was removed by exposing the PCB to a saturated solution of iron perchloride for 20 min (step 3). Next, a mask made of adhesive tape was used to coat the substrate for application of the conductive graphite ink and conductive silver epoxy. Using a small brush, the CE and the pseudo-RE were produced (step 4). Afterwards, the SPEs were heated at 150 °C for 45 min to remove the solvent, aiming to reduce the electrical resistance of these materials. Then, a thin layer of epoxy resin (Araldite®, Brazil) was used to electrically isolate the contacts from the SPEs (step 5). After drying the resin for 4 h, the electrodes were appropriately cut. Applying this procedure, with a single board of 20×20 cm^2, 65 SPEs were produced. The dimensions of the SPEs were as follows: WE: 12.6 mm^2, CE: 28.2 mm^2, pseudo-RE: 9.0 mm^2, width: 12.0 mm, length: 40.0 mm.

The CE based on graphite ink and the pseudo-RE based on conductive epoxy resin were manually applied. On the other hand, the amounts employed were quantitatively measurements using an analytical balance. The masks made of adhesive tape were based on the CE and RE dimensions that cover just a limited area under the SPE. However, the more critical step to produce the SPE-BiFE consists in the electrodepositing of bismuth film on the copper substrate. In this step, the geometric area was delimited through the copper substrate produced by screen-printed technology and the amount of bismuth film was controlled by chronoamperometric technique.

2.4. Thermostated electrochemical flow cell

In Fig. 2A, the developed EFC is shown, which was composed of a poly(methyl methacrylate) block, which was machined to allow coupling of a thermoelectric cell based on Peltier effect (TEC-Peltier), an LM35 temperature sensor and a SPE for flow electroanalytical analysis. In Fig. 2B, the EFC was filled from the bottom up, employing a μP for one of the channels of 0.05 mm i.d. that was at a tangent to the circumference base. The solution filling the base of the EFC (1.77 cm^2) comprised of TEC-Peltier, covering a 2.0 mm thick Teflon® magnetic bar with (2.0 mm width × 6.0 mm length) (not shown), the SPE, and the temperature sensor, which required 700 μL in total. There was no direct contact between the TEC-Peltier and the SPE, since a 3.0 mm layer of solution was located between them. The internal volume of 700 μL was small enough to allow procedures with detection in flow or to stopped-flow technique. Fig. 2C shows the set-up where a stainless steel tube was used in place of the Tygon® tube (3.0 mm i.d.) as the external CE. In addition, an Ag/AgCl (3.0 mol L^{-1} KCl) external RE situated perpendicular to the upper face of the EFC can also be used instead. Thus, the EFC can be used with the SPE with three electrodes embedded in the same device, or can be used with an external RE and a CE from the SPE; as a result, the EFC has hybrid characteristics.

The seven 0.8 mm i.d. PTFE blue tubes penetrate into the EFC, but before reaching the inner circumference, they are reduced in length by 2 mm and 0.05 mm i.d., thereby preventing each tube from crossing the inner circumference of the EFC.

Fig. 2B shows a 6.0 mm i.d. thermoplastic O-ring used to seal the SPE; a piece of aluminum was used to hold and press the

O-ring to seal the SPE (not shown), with a thermoplastic O-ring of 2.1 cm i.d. to seal the EFC in its base. A small magnetic bar was needed to promote the mechanical agitation during the pre-concentration step in ASV (Fig. 2C). For this, a 12 VDC motor with two magnets coupled to its axis was used and it was controlled by software. Besides the apparatus described, a heat dissipation system composed of an aluminum block and a fan was used and is shown in the figures; this was necessary to sink the heat generated in one of the faces of the TEC-Peltier. Moreover, the thermostated control of the EFC base of the TEC-Peltier was driven by a microcontrolled board that was developed for this purpose.

The internal volume of the EFC, disregarding the volumes occupied by the magnetic bar, LM35 sensor and SPE, was 970 μL. An EFC with a nominal volume of 1300 μL was projected to allow a higher dilution capacity. However, as a balance had to be maintained between the lowest amount of chemical reagents and no loss of flexibility and robustness, the model with 700 μL was used in this work.

The EFC developed shows features of the flow-batch chamber used by Honorato et al. [18] in flow-batch analysis. However, this EFC can be used in other procedures, such as FIA, SIA and MCFA, among others, as it is more versatile and appropriate for electrochemical experiments. Thus, due to the use the EFC as a chamber, the flow system is better characterized as FBA.

For more details of the EFC developed, an illustrated video in AVI format is supplied as supplementary data online.

Supplementary material related to this article can be found online at http://dx.doi.org/10.1016/j.talanta.2014.03.015.

2.5. Control of the FBA system

To pump solutions through the transmission lines in the FBA system, the solenoid μPs were used as propulsion devices to inject solutions within the EFC. For this, potential pulses of 12 V were applied at a frequency of between 1 and 10 Hz to evaluate the flow rate. The symbols (1) and (0) were adopted in Table 1 to represent the on and off states of the μPs, respectively. The solenoid of the μP has a limit time response of 80 ms to execute one pulse. Therefore, by applying 4 Hz (250 ms) for each task (ON or OFF), a complete cycle takes 0.5 s to pump a 20 μL aliquot of solution. Therefore, a flow rate of 40 μL s^{-1} or 2.4 mL min^{-1} was obtained. Also, the frequency of cycles performed was proportional to the flow rate of the pumped solutions and the number of cycles for each μP defines the total volume pumped for each one.

The electronic circuit of the actuator has a small dimension (4.0 cm × 4.0 cm) and controls the μP, SV and magnetic stirrer. It basically consists of digital control lines from the 6008 USB interface (NI®, USA), a current driver (ULN2003A), resistors, and LEDs which are used as flags (ON/OFF). Calibration tests of μPs and SV were performed using software developed in Labview®.

2.6. Thermostated EFC and FBA procedures

In Fig. 3, the FBA manifold developed to perform the on line and *ex situ* bismuth electrochemical deposition and further Pb^{2+} and Cd^{2+} ions determination by SWASV is shown.

As can be seen, when the SV1 is switched on, air is inserted into the EFC for two purposes: (1) to dry and clean the EFC, as the air bubbles are very effective for this purpose, and (2) to reduce the consumption of the supporting electrolyte, thus generating less waste. The alternative channel "drain" was commutated by switching on SV2, which was the most efficient procedure for drying and cleaning the EFC. This drain consisted of a channel of 0.05 mm present on the base of the EFC for which the solutions are discarded. As 700 μL was sufficient to fill the EFC, a combination of μPs was used in various configurations, allowing wide flexibility for the analytical procedure, such as on line dilutions, the

Table 1
Sequence of the experiments employing FBA with μP and SV.

Steps	Description	μP1	SV1	SV2	S[a]	μP2	μP3	μP4	μP5	μP6	P[b]	T (s)[c]
1	Filling the channels	1/0	1	0	0	1/0	1/0	1/0	1/0	1/0	20	10
2	Addition of Bi^{3+}	0	0	0	1	0	0	0	1/0	0	35	17.5
3	Temperature control[d]	0	0	0	1	0	0	0	0	0	0	30
4	Cyclic voltammetry	0	0	0	0	0	0	0	0	0	0	84
5	Electrochemical cleaning	0	0	0	1	0	0	0	0	0	0	10
6	Drainage/air	1/0	0	1	1	0	0	0	0	0	40	20
7	Cleaning	1/0	1	0	1	0	0	0	0	0	35	17.5
8	Drainage/air	1/0	0	1	1	0	0	0	0	0	40	20
9	Addition of Bi^{3+}	0	0	0	1	0	0	0	1/0	0	35	17.5
10	Temperature control	0	0	0	1	0	0	0	0	0	0	30
11	BiFE *ex situ* deposition	0	0	0	1	0	0	0	0	0	0	180
12	Drainage/air	1/0	0	1	1	0	0	0	0	0	40	20
13	Cleaning	1/0	1	0	1	0	0	0	0	0	35	17.5
14	Drainage/air	1/0	0	1	1	0	0	0	0	0	40	20
15	Addition of blank[e]	1/0	1	0	1	0	0	0	0	0	35	17.5
16	Addition of Pb[e]	1/0	1	0	1	1/0	0	0	0	0	1–35	0.5–17.5
17	Addition of Cd[e]	1/0	1	0	1	0	1/0	0	0	0	1–35	0.5–17.5
18	Simultaneous/Pb-Cd[e]	1/0	1	0	1	1/0	1/0	0	0	0	1–17	0.5–8.5
19	Addition of sample[e]	1/0	1	0	1	0	0	0	0	1/0	1–35	0.5–17.5
20	Temperature control	0	0	0	1	0	0	0	0	0	0	30
21	Pre-concentration	0	0	0	1	0	0	0	0	0	0	180
22	Measurements by ASV[f]	0	0	0	0	0	0	0	0	0	0	3
23	Drainage/air	1/0	0	1	1	0	0	0	0	0	40	20
24	Cleaning	1/0	1	0	1	0	0	0	0	0	35	17.5
25	Drainage/air	1/0	0	1	1	0	0	0	0	0	40	20

[a] Magnetic stirrer was always used, except for steps 1, 4 and 22.
[b] Maximum number of pulses per actioned μP.
[c] Maximum time for each step. The μP4 was used just to interference study that not was included in this experimental sequence.
[d] Activation of the TEC-Peltier for 30 s at a rate of 30 °C min^{-1}.
[e] Selection of blank solution, metal ion standard solution, or sample.
[f] SWASV for 3 s, and DPASV for 22 s.

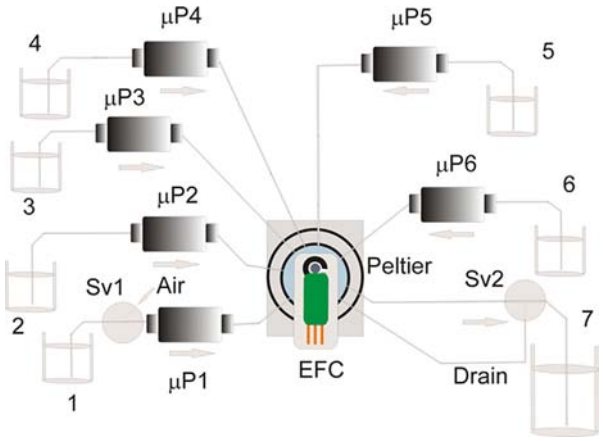

Fig. 3. The FBA manifold. The μP1 and μP5 were used to pump 20 μL per pulse of acetic acid/acetate buffer solution pH 4.0 (1) and solution of Bi^{3+} electrochemical deposition (5), respectively. The μP2, μP3, μP4, and μP6 pump 20 μL per pulse of the stock solutions of Pb^{2+} (2), Cd^{2+} (3), samples (4), and potential interference solutions (6), respectively. Moreover, waste (7), SV1, SV2: three-way solenoid valves. EFC coupled with Peltier and an alternative channel to drain solutions for disposal.

construction of analytical curves, standard addition, recovery assays, and interference studies.

To ensuring that the air bubbles do not leak through the connections in the flow manifold developed, the PTFE connections must be very well sealed, using for example PTFE tape and/or the proper ferrules based on silicon to sealing and to hold the air pressure.

2.7. Electrochemical deposition of BiFE

In previous works published by our research group [25,27], the optimization of Bi^{3+} solution for the *ex situ* electrochemical deposition of Bi under copper substrate was described, as well as the chronoamperometric parameters. A 20 mL aliquot of 0.02 mol L^{-1} Bi $(NO_3)_3 \cdot 5H_2O$ in 0.15 mol L^{-1} sodium citrate and 1.5 mol L^{-1} HCl was used. However, herein, only 700 μL was employed with an on line electrochemical deposition employing a reduction potential of −0.18 V *vs.* Ag/AgCl (pseudo-RE) for 180 s.

Once the bismuth film is electrodeposited onto copper substrate, just bismuth effectively participates in the Faradaic process. Additionally, in the presented conditions, Cu had showed a good substrate to electrodepositing bismuth, since that compound-based carbon present a poor adherence of the bismuth film. Because of this, for these substrates, just *in situ* electrodeposition is used. The bismuth film electrodeposited onto copper substrate had been characterized by scanning electron micrographs (SEM) as described in previously work [27,28].

2.8. Effect of the supporting electrolyte

The electrochemical behavior of the supporting electrolyte used in electrochemical assays for SPE based on BiFE (SPE-BiFE) was evaluated mainly by cyclic voltammetry. The following supporting electrolytes were studied: acetic acid/acetate buffer solution (0.2 mol L^{-1}, pH 4.0 and 4.5), phosphate buffer (0.2 mol L^{-1}, pH 4.0 and 5.0) and Britton-Robinson (BR) buffer (0.04 mol L^{-1}, pH 2.0, 4.0 and 6.0). The potential window, residual current, voltammetric profile and peak current were the main parameters evaluated.

2.9. Evaluation of the parameters of DPASV and SWASV

The parameters of differential pulse anodic stripping voltammetry (DPASV) and square-wave anodic stripping voltammetry (SWASV) techniques were evaluated by univariate analysis, mainly observing the anodic peak current (Ip) and profile of the voltammograms obtained.

2.10. Influence of temperature on Pb^{2+} and Cd^{2+} electrochemical response

Using the TEC-Peltier system for thermostatic control of the solutions within the EFC, *in loco* simulations of temperature were carried out by changing the temperature during Pb^{2+} and Cd^{2+} ions determinations using the SPE-BiFE. For this, standard solutions were inserted into the EFC and cooling or heating procedures were performed. On average, a period of only 30 s was necessary to obtain thermal stabilization within the EFC before experiments with ASV. The electrochemical experiments with different temperatures were performed with a precision of ±1 °C. Acetic acid/acetate buffer solution (pH 4.0) was used as the supporting electrolyte.

2.11. Operational sequence of the FBA system

To perform the operational sequence of the FBA to carry out procedures such as temperature control, *ex situ* electrochemical deposition of Bi under SPE, and further determination of electroactive metal ions, a series of steps was used, which is presented in Table 1. At each step, pulses (*P*) of each μP were performed, with each pulse representing a complete cycle of switching ON/OFF (1/0) of each μP. For the experiments, a pulse frequency of 4 Hz was used. The same methodology was adopted for SV and the magnetic stirrer (S). The Pb^{2+} and Cd^{2+} stock solutions were prepared in acetic acid/acetate buffer solution at pH 4.0 in order to minimize the effects of pH change and ionic strength of the solution and to avoid hydrolysis *via* the addition of aliquots of solutions during the on line dilution.

The following procedures were performed for on line and *ex situ* electrochemical deposition of Bi with detection by ASV. Initially, all channels of the flow system were filled with the respective solutions by switching on all μPs for 20 pulses (20 μL per pulse). Then, 700 μL of electrodeposition solution was pumped by μP5 using 35 pulses at a flow rate of 40 μL s^{-1} to fill the EFC. All flow was stopped and the μC-TEC-Peltier (TEC-Peltier driven by a microcontroller) was activated for 30 s for the thermal control of the solution at 25 ± 1 °C. Following this, a cyclic voltammogram was performed to evaluate the electrochemical deposition of bismuth film [25]. Thereafter, the SPE was electrochemically cleaned to remove BiFE by applying +0.2 V *vs.* Ag/AgCl (Pseudo-RE) for 10 s. Subsequently, the cleaning procedure was carried out. This step consists of drainage of the solution employing air bubbles by simultaneously switching on and triggering μP1 and SV2 for a flow rate of 40 μL s^{-1}, thereby discarding the solution. Then, SV1 was switched on simultaneously with μP1 for 35 pulses with SV2 switched off to drive the supporting electrolyte solution to clean the EFC system. Again, 700 μL of electrochemical deposition solution was pumped through using μP5 to fill the EFC. The temperature was controlled and chronoamperometry was performed by applying −0.18 V *vs.* Ag/AgCl for 180 s to reduce Bi^{3+} under SPE copper substrate [25]. This yielded SPE-BiFE which was ready to be used. After this, the cleaning procedures were performed and the FBA system was employed for the determination of Pb^{2+} and Cd^{2+} by ASV through the activation of proper μP (steps 15–19 in Table 1).

2.12. Potential interference by employing the SPE-BiFE with SWASV

In order to evaluate the potential interference in Pb^{2+} and Cd^{2+} determination, some cations and anions that are commonly found in natural and tap water samples were studied, employing the SPE-BiFE with SWASV and FBA approaches [10,25,26,29]. Thus, the following ions were evaluated: Na^{+}, K^{+}, Ca^{2+}, Li^{+}, Mg^{2+}, Fe^{3+}, Cl^{-}, NO_3^{-}, CO_3^{2-}, SO_4^{2-}, PO_4^{3-}. In addition, electroactive ions were studied, such as Ni^{2+}, Cu^{2+}, Al^{3+}, Hg^{2+}, Cr^{3+} and Mn^{2+}, and other compounds such as humic acid (HA) from the turf and vermicompost (1.0% (w/v)) dissolved in 0.02 mol L^{-1} $NaHCO_3$.

To perform this procedure, μP3 and μP2 were activated by 8 and 16 pulses to add aliquots of Pb^{2+} and Cd^{2+} solution into the EFC, respectively, while μP4 was used for propulsion of the solution with potential interference. The final concentrations of the analytes in the EFC were: 50.4 μg L^{-1} Cd^{2+} and 50.9 μg L^{-1} Pb^{2+}. The percentage of interference was calculated based on the difference of the Ip ($n=3$) compared to response without the interferent species. Any interfering concentrations were evaluated in ratios of 1:1, 1:10, and 1:100 (analyte: interferent).

3. Result and discussion

3.1. Calibration tests of the FBA system

Tests were performed to evaluate the minimum time required for the activation of the μPs; generally, 0.1 s or 10 Hz was employed. Moreover, 4 Hz, equivalent to a flow rate of 40 μL s^{-1}, was employed for each μP. For higher flow rates, the standard deviations were increased, possibly due to the gradual increase of the hydrodynamic impedance. However, it was noted that standard deviation lower than 4.0% were obtained ($n=6$). Additionally, according to the performed assays, the volume pumped was in close agreement with the nominal value described by the manufacturer, with a precision of 0.8% for 20 μL per pulse (20.0 ± 0.2 μL), which was reproducible over five cycles.

3.2. Sampling frequency

Using Table 1, it was possible to estimate the sampling frequency, taking into account steps 15–25. Thus, for example, the time required to complete a determination by SWASV ranged from 271.0 to 288.0 s, which was equivalent to a sampling rate of between 12 and 13 h^{-1}. For a new analytical cycle, the sequence should be initiated at any step between 15 and 19. For DPASV, a frequency between 11 and 12 h^{-1} was estimated. As can be seen, the FBA system was able to determine Pb^{2+} and Cd^{2+} ions by single or simultaneous analyses; however, the simultaneous procedure was mainly presented herein. As aforementioned, for the calculus of sampling frequency, the *ex-situ* deposition of BiFE was performed only once.

3.3. Supporting electrolyte

In Fig. S1, in the supplementary data, the cyclic voltammograms (CV) of the SPE-BiFE in different supporting electrolytes are presented. In addition, the cyclic voltammogram of Pb^{2+} ions was presented showing its reduction/oxidation electrochemical profile in different supporting electrolytes. For all cyclic voltammograms, a potential sweep rate of 50 mV s^{-1} was used. The CVs were obtained using the CE based on conductive graphite ink, the Ag/AgCl as pseudo-RE and BiFE as WE. According to the voltammograms obtained, the most suitable supporting electrolytes were acetic acid/acetate buffer and phosphate buffer at pH 4.0, and BR buffer at pH 6.0. However, based on the widest cathodic potential window, lower residual current and the profile of the oxidation peaks and reduction from the reversible system Pb^{2+}, the acetic acid/acetate buffer solution (pH 4.0) was selected [5,9].

3.4. Optimization of parameters from the DPASV and SWASV

Experiments were performed in order to determine the best parameters for DPASV and SWASV for the simultaneous determination of Pb^{2+} and Cd^{2+} ions. In the pre-concentration step, the Ip increased until a pre-concentration potential of −1.4 V, however, at −1.2 V, a better repeatability was acquired with low $H_{2(g)}$ evolution. Similarly, the Ip increase was proportional to the time applied for pre-concentration until 180 s; after this, the Ip tended to reach a plateau. To obtain a balance among the sensitivity, precision and sampling frequency, a pre-concentration potential of −1.2 V and a time of 180 s were applied using the stopped-flow technique, with the stirrer switched on, as described in Table 1. The parameters of DPV and SWV were evaluated based on maximum Ip, baseline definition, and resolution based on potential width at half-height peak ($\Delta Ep_{1/2}$), which is important for simultaneous determinations. For both pulsed voltammetry techniques, an increase in Ip was correlated with an increase of the pulse amplitude (a) and potential sweep rate (υ); however, the $\Delta Ep_{1/2}$ became wider, impairing the resolution of the voltammograms obtained. Thus, the parameters selected for DPASV were: (a) 70 mV, pulse application time (τ) of 5 ms and (υ) 50 mV s^{-1}. For SWASV, the parameters were: (a) 70 mV, step potential (ΔE) of 5 mV and frequency (f) of 70 Hz. By employing the optimized parameters, both SWASV and DPASV techniques supplied well-defined and undistorted voltammograms, as presented in supplementary data (Fig. S2). However, SWASV showed a higher Ip with narrower $\Delta Ep_{1/2}$ than DPASV, and was therefore used for further electrochemical experiments.

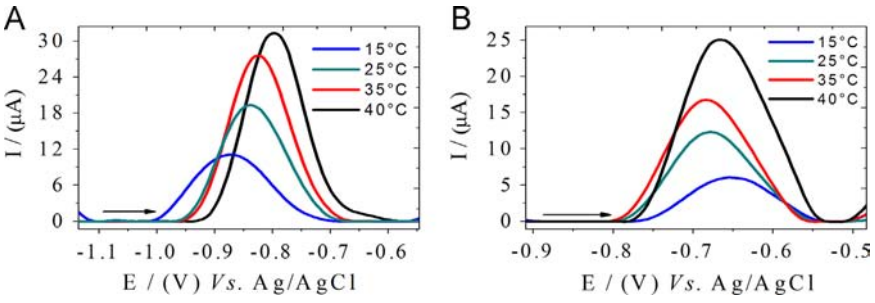

Fig. 4. Evaluation of the effect of temperature on the voltammetric determination by SWASV for Cd^{2+} (A) and Pb^{2+} (B) using SPE-BiFE. Parameters for SWASV: (a) 70 mV, (ΔE) 5 mV and (f) 70 Hz. E_{dep} and t_{dep} were −1.2 V and 180 s, respectively. Acetic acid/acetate buffer pH 4.0 was used as supporting electrolyte.

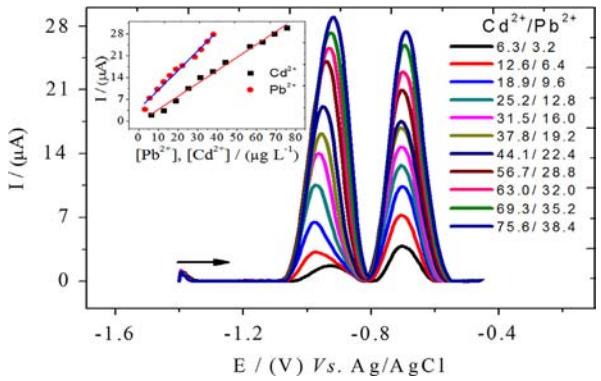

Fig. 5. Simultaneous analytical curves employing SWASV and SPE-BIFE for the determination of Pb^{2+} and Cd^{2+} ions. SWASV parameters: *a* (mV)=70, ΔE (mV)=5 and ƒ (Hz)=70 Hz, potential and time of electrochemical deposition were −1.2 V and 180 s, respectively.

3.5. Influence of temperature on the SWASV of Pb^{2+} and Cd^{2+}

Aliquots of 160 and 140 μL stock solutions of Pb^{2+} (111.3 μg L^{-1}) and Cd^{2+} (220.3 μg L^{-1}) were pumped and added to the thermostated EFC to evaluate the effect of temperature on the SWASV experiments. When the temperature of the system increased, a displacement in the anodic peak potential and an increase in Ip were observed, as shown in Fig. 4. The changes in temperature modified the standard potential and mass transport of the species as well as the viscosity of the solution [24]. The change in the mass transport was a consequence of the shift in the diffusion coefficient. Thus, in general, this process increases the peak current when the temperature is raised [22,23]. In fact, Ip undergoes a maximum variation between −42.1% (*T*=15 °C) to 63.1% (*T*=40 °C) and –50.4% (*T*=15 °C) to 102.4% (*T*=40 °C) for the Cd^{2+} and Pb^{2+} ions, respectively, using the Ip at 25 °C as a reference. The change in the magnitude of Ip is a major problem that affects *in loco* electrochemical analysis, which is subject to abrupt changes in temperature. Therefore, the remaining trials were conducted with the temperature controlled at 25 ± 1 °C.

3.6. SPE-BiFE with FBA approach used to construct the analytical curves

Analytical curves were constructed by the simultaneous addition of the stock solutions of Pb^{2+} and Cd^{2+} ions into the EFC by appropriate multicommutation of μP2 and μP3, according to step 18 in Table 1. The analytical curves were linear by applying successive pulses from 1 to 12 for each μP. To fill the EFC, for each pair of aliquot of Pb^{2+} and Cd^{2+} solution added, aliquots of acetic acid/acetate buffer solution (pH 4.0) were added, triggering the μP1 and SV1 according to Table 1. As shown in Fig. 5, the construction of analytical curves for the simultaneous determination of Pb^{2+} and Cd^{2+} ions was performed and the major results are summarized in Table 2.

Observing the data presented in Table 2, it can be seen that satisfactory repeatabilities were obtained using the FBA system with SWASV with relative standard deviations (RSD) of 2.9% and 4.1% for 28.6 μg L^{-1} Pb^{2+} and 63.0 μg L^{-1} Cd^{2+}, respectively. Moreover, linear ranges from 3.20 to 38.4 μg L^{-1} and from 6.30 to 75.6 μg L^{-1} for these ions were respectively obtained. Additionally, good analytical results were achieved, supplying LDs of 0.10 and 0.60 μg L^{-1} (*S*/*N*=3). The repeatability of the method employed was evaluated by testing the analytical sensitivity with four concentrations of standard solution of Cd^{2+} and Pb^{2+} ions with *n*=3, constructed for each of the five *ex-situ* SPE-BiFE produced. Thus, RSD of 6.5% and 8.0% were obtained. The lifetime of each BiFE was also found to be approximately 70–80 measurements.

Table 2
Main results obtained for SPE-BiFE–FBA with SWASV.

Analytical performance parameters	Pb^{2+}	Cd^{2+}
Sensitivity (μA/μg L^{-1})	0.71	0.42
Coefficient of regression (*r*)	0.990	0.992
Limit of detection (μg L^{-1})	0.10	0.60
Limit of quantification (μg L^{-1})	0.33	2.00
Linear range (μg L^{-1})	3.20–38.4	6.30–75.6
Repeatability (RSD)[a]	2.9%/28.6	4.1%/63.0

[a] Based on RSD (*n*=3)/analyte concentration in (μg L^{-1}).

After this lifetime, the bismuth film was removed by electrochemical treatment and a new bismuth film was again deposited onto the copper substrate (SPE-BiFE).

3.7. Potential interference by employing the SPE-BiFE with SWASV

Among all of the evaluated potential interference, only the Cu^{2+} and Hg^{2+} ions with concentrations higher than 50.4 and 50.9 μg L^{-1} (refer to concentration ratio higher than 1:1) generated interference levels greater than 10%. Therefore, these concentrations were considered the maximum tolerated for the proposed electrochemical method. In the case of Cu^{2+} ions, these interferences are possibly associated with the formation of intermetallic compounds with Cd and Pb metals in the active sites on the surface of the SPE-BiFE. In the case of Hg^{2+} ions, the interference encountered can be attributed to the competition reactions between Hg^{2+} ions and the active sites of BiFE regarding the Cd^{2+} and Pb^{2+} ions that are free in solution, or even blocking the active sites of the BiFE surface, as discussed in some previous studies [7,12,30,31]. Moreover, the HA concentration tolerated was calculated to be 1.0×10^{-2}% (w/v). Higher concentrations of HA generated interferences levels higher than 10% in the determination of Cd^{2+} and Pb^{2+} ions, since HA is known to be a macromolecule with a high capacity for complexation. However, this interference can be removed by precipitation and centrifugation of HA in acid solution prior to measurements [32].

3.8. Recovery and certified method employing the FBA and the SPE-BiFE

The samples were acquired from the Monjolinho Lake (São Carlos, Brazil) (A), wastewater from the petrochemical (Petrobras, Brazil) (B), and tap waters from Lisbon, Portugal (C) and Alicante, Spain (D). The recovery test was carried out to evaluate the accuracy of the proposed electrochemical flow method. In samples A and B, the recovery studies were carried out by adding Pb^{2+} and Cd^{2+}; in sample C only Pb^{2+} and in sample D only Cd^{2+} were added, according to Table 3.

Based on the data presented in Table 3, the recovery tests were satisfactory, ranging from 90.1 to 111.0, thereby suggesting that potential interfering species were not found or were not present at concentrations above those considered tolerable, as previously discussed.

After the recovery tests, the accuracy of the electrochemical method was validated employing a certified river water (1643e Trace Elements in Water, NIST). According to NIST, the certified water has the following concentrations of Cd^{2+} and Pb^{2+} ions: 6.58 ± 0.073 μg L^{-1} and 19.63 ± 0.21 μg L^{-1}, respectively. After a proper calibration employing the standard addition method, the concentrations found were: 6.8 ± 0.3 μg L^{-1} and 18.9 ± 0.8 μg L^{-1}, respectively. Supported by the data, relative errors less than 4.0% for *n*=5 and the *t*-unpaired values of 1.47 and 1.83 were

Table 3
Results of recovery test.

[a]S	Added ($\mu g\ L^{-1}$)		Found ($\mu g\ L^{-1}$)		Recovery (%)	
	Pb^{2+}	Cd^{2+}	Pb^{2+}	Cd^{2+}	[b]R_1	[c]R_2
A	6.4	12.6	7.0 ± 0.5	13.0 ± 0.5	109.8	103.0
	12.7	25.2	13.3 ± 0.2	24.1 ± 0.7	104.5	95.6
	19.1	37.8	18.9 ± 0.8	36.5 ± 0.4	99.3	109.3
B	3.2	6.3	3.2 ± 0.1	5.7 ± 0.5	101.6	90.1
	9.5	31.5	10.6 ± 0.5	32.0 ± 0.9	111.0	101.9
	22.2	113.0	20.1 ± 0.6	114.0 ± 0.8	90.5	108.4
C	6.4	–	6.6 ± 0.2	–	104.6	–
	15.9	–	16.6 ± 0.8	–	109.6	–
	25.4	–	27.9 ± 0.6	–	103.6	–
D	–	12.6	–	11.8 ± 0.9	–	93.3
	–	25.2	–	27.6 ± 0.8	–	109.5
	–	37.8	–	38.5 ± 0.5	–	106.6

[a] Samples.
[b] Percentage of recovery (%) for Pb^{2+}.
[c] Percentage of recovery (%) for Cd^{2+}.

Table 4
Comparison among the results from the present work and others found in the literature.

BiFE	Flow parameters			Pb^{2+}		Cd^{2+}		[e]Sub
[a]Refs.	Flow	[b]F (h^{-1})	[c]V (μL)	[d]L ($\mu g\ L^{-1}$)	LD ($\mu g\ L^{-1}$)	[d]L ($\mu g\ L^{-1}$)	LD ($\mu g\ L^{-1}$)	
[14]	SIA	5.5	6000	0.5–15.0	0.01	0.5–15.0	0.01	[f]CNT
[12]	SIA	14	1440	0.0–70.0	0.89	0.0–70.0	0.69	[g]C
[33]	SIA	10–15	1440	2.0–100.0	0.80	2.0–100.0	0.80	[f]CNT
[8]	[h]FIA-SIA	15–20	1000	0.0–70.0	1.00	0.0–56.0	2.00	[i]GC
[13]	[j]MSFIA	14	1300	–	–	5.0–60.0	0.79	[g]C
[k]Pr	FBA	12–13	700	3.2–38.4	0.10	6.3–75.6	0.60	[l]Cu

[a] References.
[b] Sampling frequency.
[c] Reagent consumption per analysis.
[d] Linear range.
[e] Substrate for the BiFE deposition.
[f] Carbon nanotubes.
[g] Carbon.
[h] Hybrid system FIA and SIA.
[i] Glassy carbon.
[j] Multi-syringe flow injection analysis.
[k] Present work.
[l] Copper.

respectively obtained. These values are in close agreement at a confidence level of 95%, *t*-test (4, 95%)=2.78.

Based on these results, particularly in terms of analytical performance parameters, recovery and accuracy tests, the electrochemical method developed showed good sensitivity required for the quantification of Pb^{2+} and Cd^{2+} ions in water samples with satisfactory accuracy, either for individual or simultaneous determinations. In Table 4, the analytical performance of the developed electrochemical method and others described in the literature are presented for comparison.

The proposed procedures showed satisfactory results compared with those previously reported, and since 700 μL of reagent was consumed, an analytical frequency of 13 h^{-1} can be achieved with low LDs. Moreover, the low waste generation of only 700 μL per determination and the on line temperature control of the solutions are features of the developed electrochemical method that can be very useful for the *in loco* electrochemical determinations, not only for the determination of metal ions, but also for organic compounds [25].

4. Conclusions

The thermostated EFC system afforded an analytical procedure that was fully automated, with multitasking and which produced measurements with controlled temperature. In fact, on line procedures such as the electrochemical deposition of Bi, cleaning of the SPE, recovery studies, analytical curves, interference, and pre-concentrations were performed without physical modification of the EFC and were all fully automated. Furthermore, the detection with a stopped flow for analyte determination was performed using SWASV with a sampling frequency of 13 h^{-1}, with a consumption of 700 μL of reagents per determination. Moreover, the LDs and LQ_S for Pb^{2+} and Cd^{2+} were compatible with those achieved by employing similar methods which have been previously reported in the literature.

Acknowledgments

The authors acknowledge the Conselho Nacional de Pesquisa Científica e Tecnológica (CNPq), Coordenação de Aperfeiçoamento de Pessoal de Nível Superior (CAPES), and Fundação de Amparo à Pesquisa do Estado de São Paulo (FAPESP), Proc. No. 2010/11690-0 and 2013/14993-1 for the financial support and scholarships supplied. We thank T. B. Guerreiro for your help designing Fig. 2 and the video shown in the supplementary data section.

Appendix A. Supporting information

Supplementary data associated with this article can be found in the online version at http://dx.doi.org/10.1016/j.talanta.2014.03.015.

References

[1] R. Desai, M.M. Villalba, N.S. Lawrence, J. Davis, Electroanalysis 21 (2009) 789–796.
[2] T. Noyhouzer, D. Mandler, Electroanalysis 25 (2013) 109–115.
[3] F. Rueda-Holgado, E. Bernalte, M.R. Palomo-Marin, L. Calvo-Blazquez, F. Cereceda-Balic, E. Pinilla-Gil, Talanta 101 (2012) 435–439.
[4] DropSens, ⟨http://www.dropsens.com/en/screen_printed_electrodes_pag.html⟩.
[5] A. Economou, Anal. Chim. Acta 683 (2010) 38–51.
[6] E.A. Hutton, B. Ogorevc, S.B. Hocevar, F. Weldon, M.R. Smyth, J. Wang, Electrochem. Commun. 3 (2001) 707–711.
[7] J. Wang, J.M. Lu, U. Anik, S.B. Hocevar, B. Ogorevc, Anal. Chim. Acta 434 (2001) 29–34.
[8] A. Economou, A. Voulgaropoulos, Talanta 71 (2007) 758–765.
[9] I. Svancara, C. Prior, S.B. Hocevar, J. Wang, Electroanalysis 22 (2010) 1405–1420.
[10] D.Q. Huang, B.L. Xu, J. Tang, L.L. Yang, Z.B. Yang, S.P. Bi, Int. J. Electrochem. Sci. 7 (2012) 2860–2873.
[11] L.S. Andrade, M.C. de Moraes, R.C. Rocha-Filho, O. Fatibello-Filho, Q.B. Cass, Anal. Chim. Acta 654 (2009) 127–132.
[12] S. Chuanuwatanakul, W. Dungchai, O. Chailapakul, S. Motomizu, Anal. Sci. 24 (2008) 589–594.
[13] C. Henriquez, L.M. Laglera, M.J. Alpizar, J. Calvo, F. Arduini, V. Cerda, Talanta 96 (2012) 140–146.
[14] B. Ninwong, S. Chuanuwatanakul, O. Chailapakul, W. Dungchai, S. Motomizu, Talanta 96 (2012) 75–81.
[15] A. Morales-Rubio, B.F. dos Reis, M. de la Guardia, Trends Anal. Chem. 28 (2009) 903–913.
[16] C.K. Zacharis, P.D. Tzanavaras, A.N. Voulgaropoulos, B. Karlberg, Talanta 77 (2009) 1620–1626.
[17] B.F. Reis, M.F. Gine, E.A.G. Zagatto, J.L.F.C. Lima, R.A.S. Lapa, Anal. Chim. Acta 293 (1994) 129–138.
[18] R.S. Honorato, M.C.U. de Araujo, R.A.C. Lima, E.A.G. Zagatto, R.A.S. Lapa, J.L.F.C. Lima, Anal. Chim. Acta 396 (1999) 91–97.
[19] S. Assmann, C. Frank, A. Koertzinger, Ocean Sci. 7 (2011) 597–607.
[20] R.S. Lima, V.B. dos Santos, T.B. Guerreiro, M.C.U. de Araujo, E.N. Gaiao, Quim. Nova 34 (2011) 135–139.
[21] A. Kausaite-Minkstimiene, V. Mazeiko, A. Ramanaviciene, A. Ramanavicius, Sens. Actuators, B 158 (2011) 278–285.
[22] J. Krejci, Z. Sajdlova, T. Marvanek, Sensors 10 (2010) 6821–6835.

[23] M. Jasinski, P. Grundler, G.U. Flechsig, J. Wang, Electroanalysis 13 (2001) 34–36.
[24] A. Nosal-Wiercińska, Cent. Eur. J. Chem. 12 (2014) 213–219.
[25] L.C.S. de Figueiredo-Filho, V.B. dos Santos, B.C. Janegitz, T.B. Guerreiro, O. Fatibello-Filho, R.C. Faria, L.H. Marcolino, Electroanalysis 22 (2010) 1260–1266.
[26] L.C.S. de Figueiredo-Filho, B.C. Janegitz, O. Fatibello-Filho, L.H. Marcolino, C.E. Banks, Anal. Methods 5 (2013) 202–207.
[27] L.M.S. Nunes, R.C. Faria, Electroanalysis 20 (2008) 2259–2263.
[28] L.C.S. de Figueiredo-Filho, D.C. Azzi, B.C. Janegitz, O. Fatibello-Filho, Electroanalysis 24 (2012) 303–308.
[29] H. Xu, L.P. Zeng, D.K. Huang, Y.Z. Man, L.T. Jin, Food Chem. 109 (2008) 834–839.
[30] A. Manivannan, R. Kawasaki, D.A. Tryk, A. Fujishima, Electrochim. Acta 49 (2004) 3313–3318.
[31] C.R.T. Tarley, V.S. Santos, B.E.L. Baêta, A.C. Pereira, L.T. Kubota, J. Hazard. Mater. 169 (2009) 256–262.
[32] V.B. dos Santos, T.B. Guerreiro, R.C. Faria, O. Fatibello-Filho, W.T. Suarez, Quim. Nova 35 (2012) 802–807.
[33] U. Injang, P. Noyrod, W. Siangproh, W. Dungchai, S. Motomizu, O. Chailapakul, Anal. Chim. Acta 668 (2010) 54–60.